Aseismic design and analysis of Er-Tan arch dam

Chuhan Zhang & Guanglun Wang
Tsinghua University, Beijing, People's Republic of China

ABSTRACT: The aseismic design and analysis of a 240m high arch dam Er-Tan are outlined for evaluating the dam safety against earthquakes. The major aspects include: The selection of the Design Earthquake, dam and reservoir interactions, the effects of dam shape on dynamic response. Comparisons between the responses by a standard response spectrum given in Chinese Specification and Park Field accelerogram of June 27, 1966, as well as the final conclusions concerning the dam safety evaluations.

1. INTRODUCTION

Er-Tan is a 240-meter high, double-curved arch dam proposed to be built on the Ya-Long River, Sichuan Province of southwest China. The installation power capacity of the project is estimated to be 3 billion watts. The total water storage capacity of the reservoir is about 5.8 billion cubic meters. The dam has a crest length of 700 meters and a maximum thickness at the bottom of 70 meters (Fig.1). The dam is to be located on a relatively stable block surrounded by several area tectonic faults and the rock formation at the dam site is composed of Permian system basalt and secondarily intruded syenite and gabbro. The seismic intensity at the dam site designated as MM VIII equivalent to peak acceleration of 0.2g is considered as the Design Basis Earthquake. A standard response spectrum based on the Chinese Specification of Earthquake Resistant Design for Hydraulic Structures and a selective earthquake time history are used in the analysis. A comprehensive study involving dam and foundation and reservoir interactions was conducted by using the finite element program-revised ADAP-TH86. Two alternatives of arch dam layout, namely, three-center circular arch and parabolic arch were analyzed for comparison. Finally, the parabolic arch was chosen for construction. This paper summarizes the major aspects of the aseismic design and analysis of the dam.

2. SEISMIC ACTIVITIES AND THE SELECTION OF THE DESIGN EARTHQUAKE

The fundamental seismic severity of the Er-Tan Dam site depends mainly on the influence of seismic activities of the outside surrounding area rather than that of the site itself. From regional geological investigations and seismic history records and distributions of currently occurring of minor shakings, we have found three major faulting belts which have significant influence on the site intensity (Fig.2) (Chengdu Design and Exploration Institute of Water Conservancy & Electrical Power). The historical events of strong earthquakes along those belts are summarized in Table 1 and also shown in Fig. 2. Some comments can be made with regard to seismic activities of the major faulting belts.

(1) Jinghe-Qinghe Faulting Belt has a faulted area width of 8-10km. A historical seismic event reaching Ms=6.7 occurred on January 19, 1467 with an epicenter intensity up to MM VIII. The nearest distance from the fault to the site is approximately 45 km and the dam site is on the short axis direction of intensity attenuation. It is concluded that the maximum effects due to this fault movement on the site intensity would be MM VI.

(2) Huaping-Dukou Implicit Faulting Belt has a characteristic of old base rock cracking, and several strong earthquakes up to Ms 5.5 to 6.0 occurred in history. The distance of 45 km from the fault to the site tends to attenuate the site in-

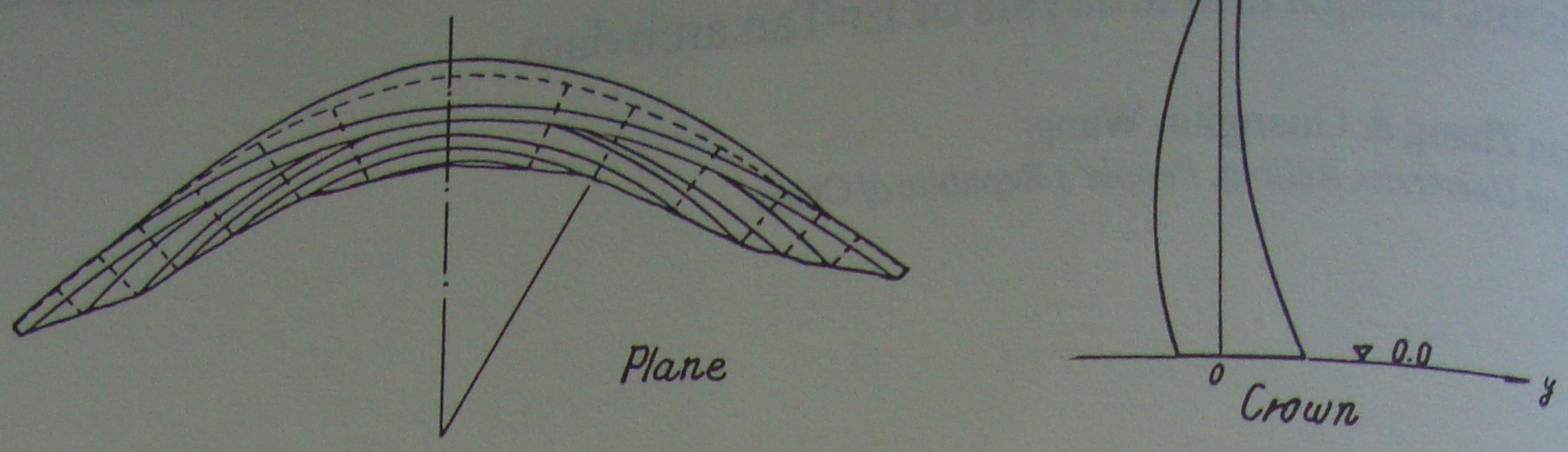

Figure 1. Layout and crown section of Er-Tan arch dam

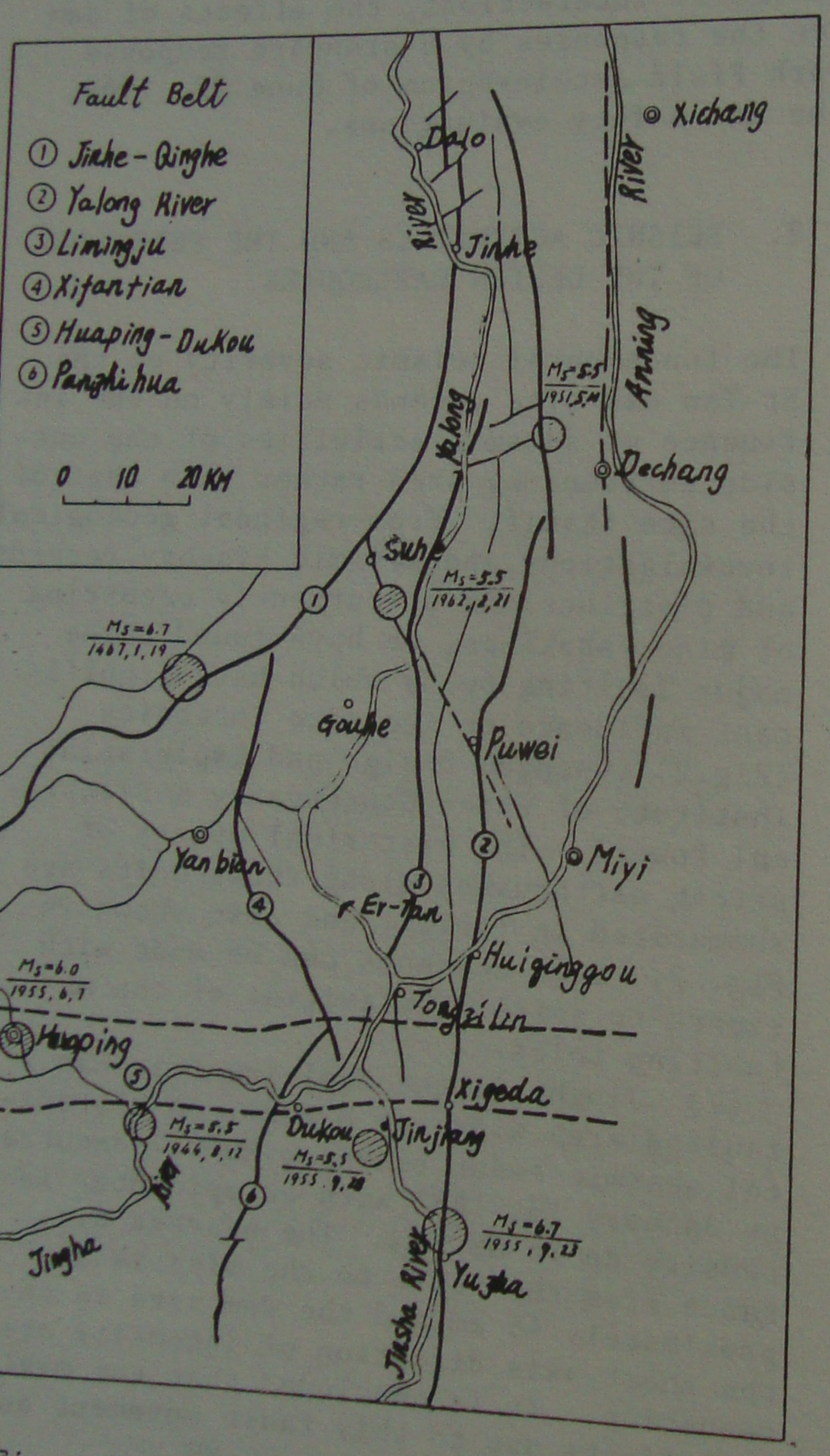

Figure2. Er-Tan area tectonic faults and historical epicenters(Ms≥5.5)

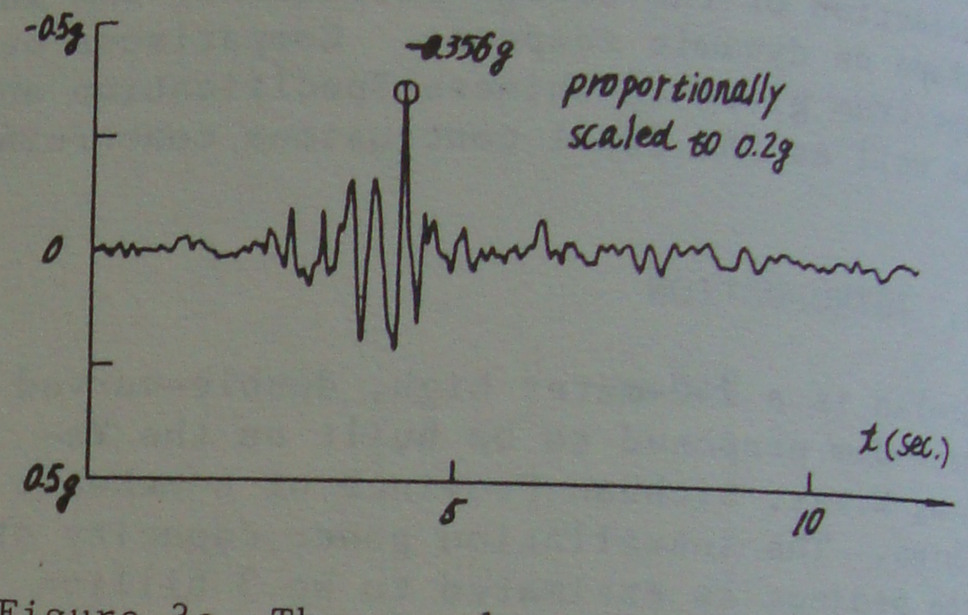

Figure 3a. The accelerogram of the Park Field earthquake on June 27, 1966

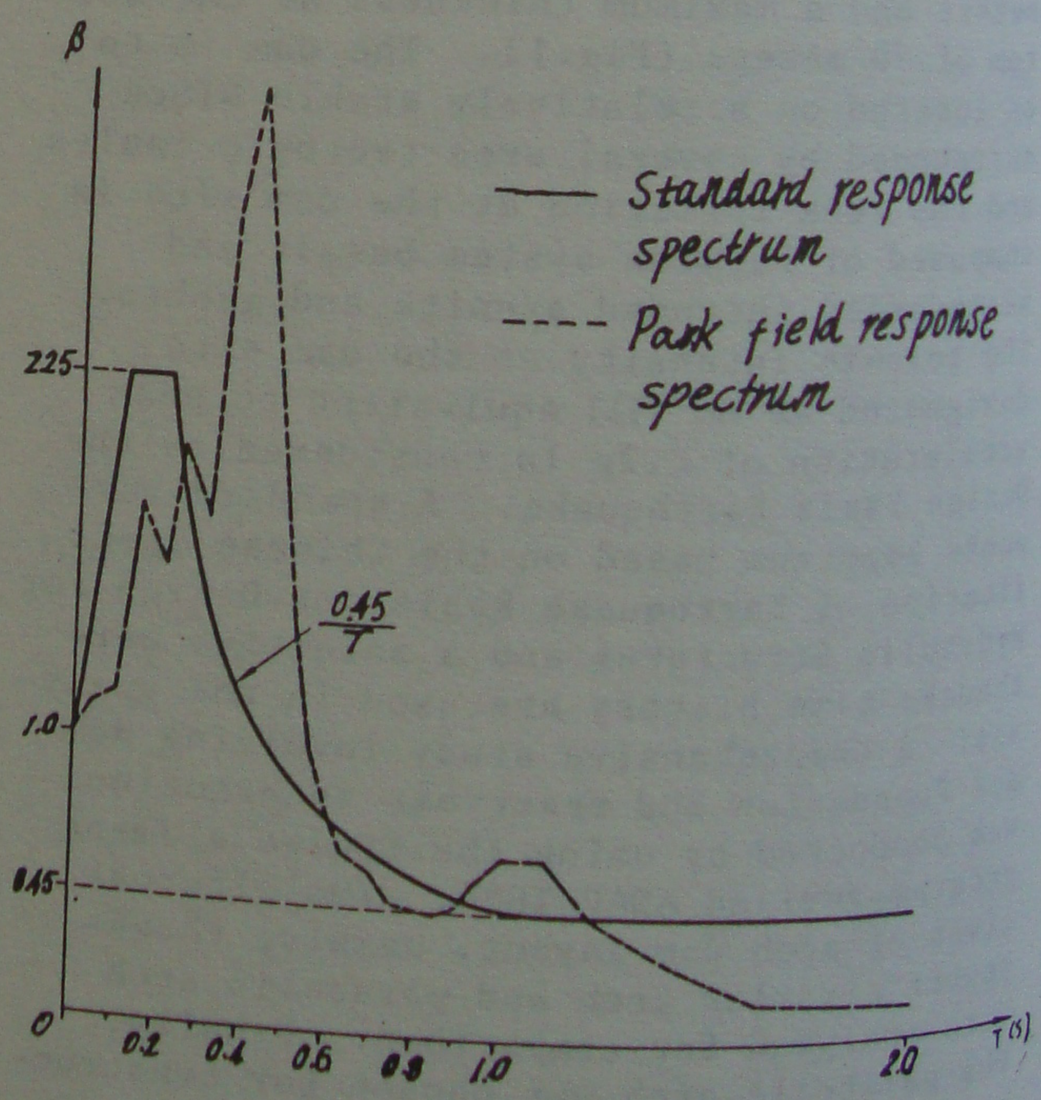

Figure 3b. Response spectra for analysis of Er-Tan arch dam

Table 1. Historical events of strong earthquakes (Ms ≥ 5.5)

No.	Date	Location	Faulting Belt	Magnitude	Intensity of epicenter	Distance to Er-Tan Dam site (KM)
1	Jan.19,1467	Yanbian Qinghe	Jinghe-Qinghe	6.7	VIII	45
2	Aug.12,1944	Dukou	Huaping-Dukou	5.5	VII	45
3	May 10,1951	Dechang	Yalong River	5.5	VII	75
4	June 7,1955	Huaping	Huaping-Dukou	6.0	VIII	54
5	Sept.23,1955	Yuzha	Yalong River	6.7	IX	50
6	Sept.28,1955	Laze	Yalong River	5.5	VII	44
7	Feb.27,1962	Suhe	Suhe	5.5	VII	48

tensity, making it not greater than MM VII.

(3) Yalong River Faulting Belt. A rather strong tectonic movement of this area causes a frequent occurrence of minor earthquakes and evident deformations of the rock mass. Several strong earthquakes occurred in history, especially a Ms=6.7 strong shaking with epicenter intensity of MM IX in 1955 at Yuzha. It is estimated the effects due to this area fault on the site intensity would be MM VII.

In addition to the three afore mentioned major fault areas there are still other local and less active faulting belts, such as Suhe Faulting Belt and Xi Fan Tian Faulting Belt, shown in Fig.2. None of them would cause an intensity of seismic shaking greater than MM VI.

(4) Reservoir impounding induced earthquakes. The shape of Er-Tan Reservoir is a long and narrow valley type. Along the length of the back water of 145 km, no active fault is found within 45km of the site. A few active faults beyond 45km will cause an earthquake intensity at the site not greater than MM VII, which is equivalent to the effect of tectonic fault shakings.

From the investigations, the fundamental intensity of the dam site is designated as MM VII. Since the Er-Tan dam and power plant are of crucial importance to the area, the Design Basis Earthquake requires an intensity of MM VIII to be considered for the design. Based on the Chinese Specification for Hydraulic Structures to Resist Earthquakes, the maximum peak acceleration of 0.2g and a standard response spectrum shown in Fig.3 are used in the analysis.

For the purpose of safety checking, the time history of the Park Field earthquake on June 27, 1966 was chosen as the input, because no real earthquake record is available for the Er-Tan Dam site. The response spectrum of Park Field earthquake is also plotted in Fig.3. As shown in Table 2, both Er-Tan and Park Field have a similar earthquake magnitude of Ms=6.5. The difference between the two sites is that the Er-Tan has a longer epicenter distance than the Park Field. It seems reasonable to proportionally scale the peak acceleration 0.356g to 0.2g considering the longer distance attenuation effect so as to make the comparison with the standard response spectrum result more consistent.

Table 2. Comparison between Er-Tan and Park Field events

	Er-Tan	Park Field
Magnitude	6.5	6.5
Epicenter distance (KM)	45	22
Maximum acceleration(g)	0.2 (designed)	0.356 (recorded)

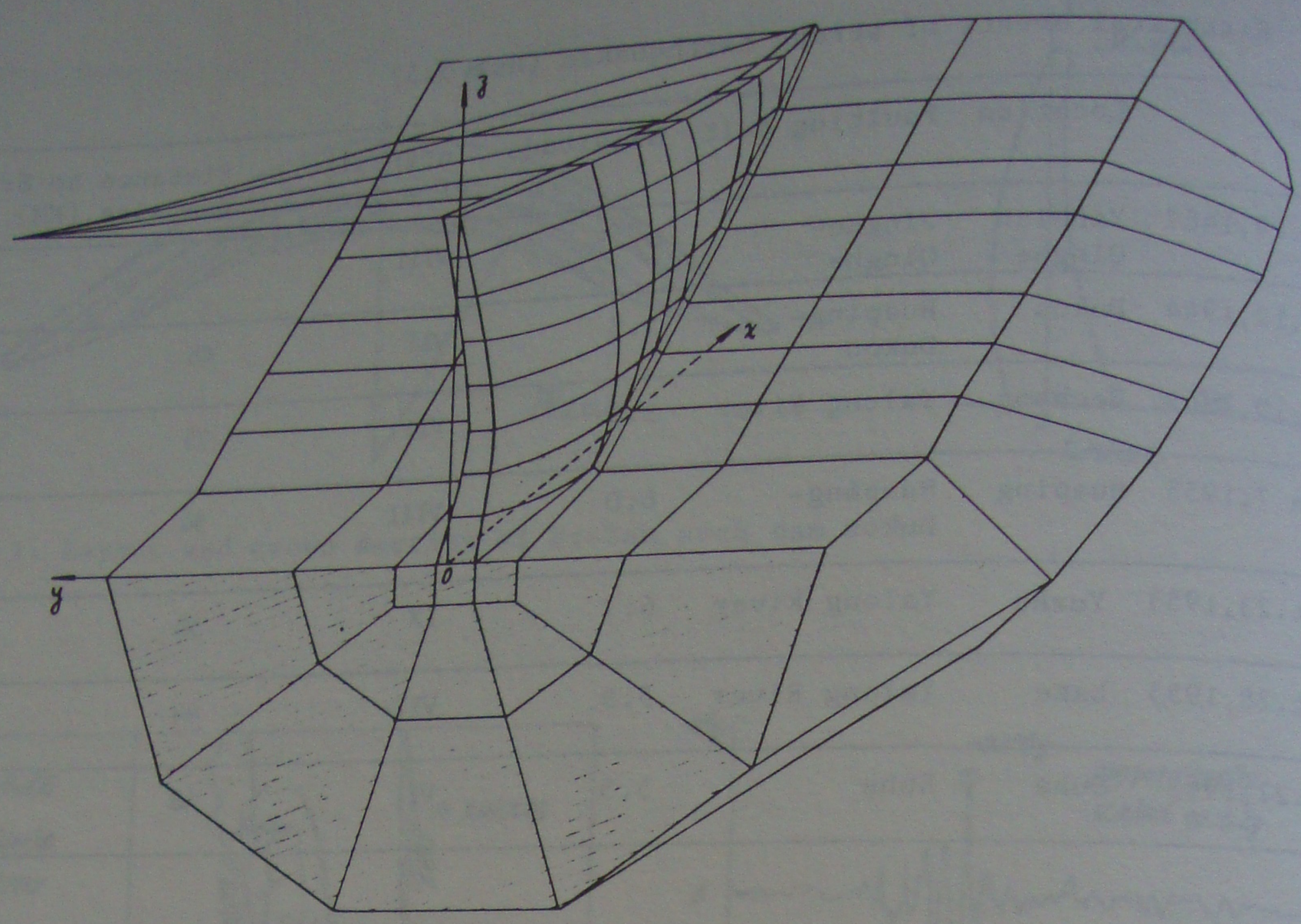

Figure 4. The finite element discretization of Er-Tan arch dam and foundation

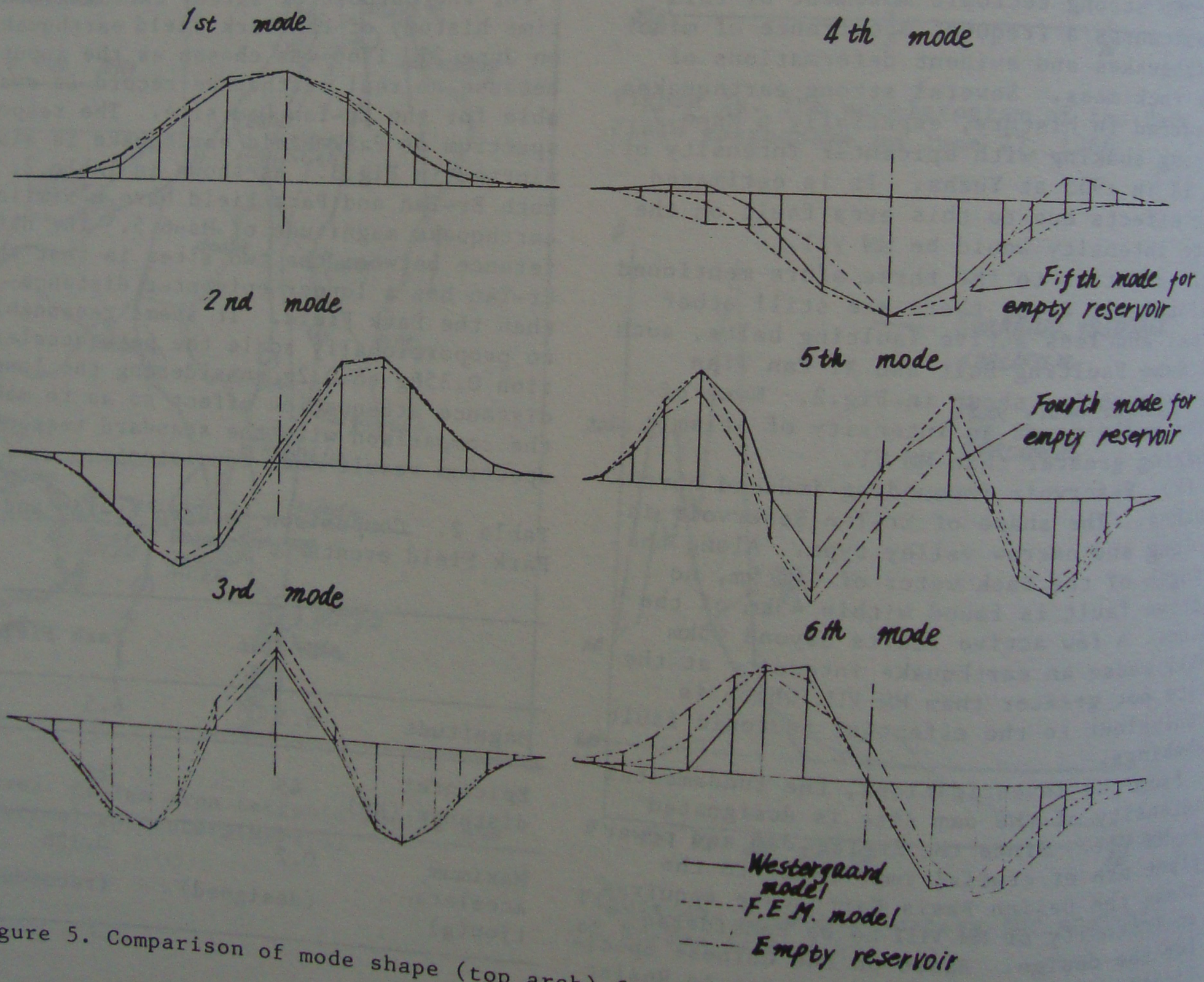

Figure 5. Comparison of mode shape (top arch) for different reservoir models

3. MATHEMATICAL MODEL AND DISCRETIZATION

The ADAP program developed by R. Clough (Clough et al. 1973) was extended by the authors to consider parabolic arch dams and was used in the analysis. Thick shell and 3-D elements were used to model the dam and foundation respectively. The dam is discretized into 8 horizontal layers and 16 columns with a total of 72 shell elements. The rock foundation which extends to one dam height H in each direction is discretized into 128 3-D elements (Fig.4). The dynamic modulus of the concrete is assumed to be 3.15×10^6 T/m^2, which is equivalent to 1.5 times the static value. The dynamic modulus of the rock foundation varies from 0.9×10^6 T/m^2 to 3.15×10^6 T/m^2 for different layers based on the results of geological investigations. The specific gravity of 2.4 T/m^3 and poisson's ratio of 1/6 for concrete are assumed. The foundation rock is modelled as a massless spring to take the foundation stiffness into account without causing a wave propagation effect from base rock to dam and foundation interface. In addition to earthquake dynamic analysis, static analysis including hydrostatic pressure, dead load and temperature change, was also carried out, but no detail on static results is presented here for the limited pages.

4. DAM AND RESERVOIR INTERACTIONS

The Westergaard added mass model and finite element discretization are used to evaluate hydro-dynamic effects on dam response. The formulations of two reservoir models are briefly described as follows:

4.1 Westergaard reservoir

Extending the Westergaard added mass formula to 3-D arch dam conditions, the dynamic fluid pressure Pi acting at point i of the dam surface has the form:

Where
$$P_i = \alpha_i \lambda_i \ddot{V}_i^t \qquad (1)$$

$$\alpha_i = \frac{7}{8} \rho \sqrt{H_i (H_i - Z_i)}$$

λ_i is the direction consine vector at point i.

ρ is the fluid density.

H_i represents the depth of the reservoir section considered.

Z_i represents the height of point i above the dam base.

$\ddot{V}_i^t$ is the total acceleration at point i.

Using the virtual work principle to obtain nodal equivalent load, the added mass for point i can be derived as follows:

$$Ma_i = \alpha_i A_i \lambda_i^T \lambda_i \qquad (2)$$

where Ai is the area contributions of elements surrounding nodal point i.

4.2 Finite element reservoir

The reservoir was discretized into 16-node 3-D elements and the length of the reservoir was assumed to be three times the dam height. Again the fluid was assumed to be incompressible; thus the added mass concept can still be appropriate to describe the interaction behavior. The formulations for finite element reservoir are described elsewhere (Clough, 1982) and need not be repeated here.

For the three-center circular arch alternative, comparisons between the two reservoir models and dry dam are shown in Table 3 and Figs 5-6.

Table 3. Frequencies from different reservoir models (HZ)

Mode No.	Empty reservoir	Westergaard reservoir	F E M reservoir
1	1.70	1.26	1.37
2	1.78	1.35	1.47
3	2.50	1.94	2.18
4	3.43	2.50	2.71
5	3.46	2.69	3.09
6	3.81	3.20	3.67

Results shown in Table 3 demonstrate that the frequencies calculated from two reservoir models are significantly reduced due to the fluid and structure interaction effects. For the first six frequencies, the Westergaard model gives a frequency reduction of 20-25% while the reduction for the finite element model is 15-20%, both compared with the empty reservoir condition. For the first six mode shapes, Fig.5 shows a similar pattern has been obtained for empty and full reservoir conditions and also for the two reservoir models. However, one point needed to be noticed is that the fourth and fifth modes for dry dam reverse their mode sequence for full reservoir conditions because the two frequencies are too close to each other. For the displacement response of the dam crest under the input of the standard response spectrum (Fig.6) the Westergaard model shows a greater fluid influence on dam response. From the results we may conclude that the

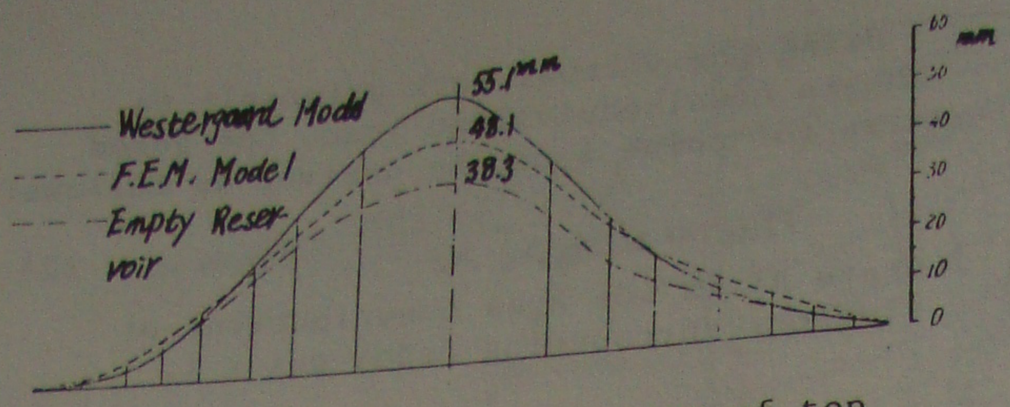

Figure 6. Upstream displacements of top arch due to upstream component of the standard response spectrum $(\ddot{v}_g)_{max}$=0.2g

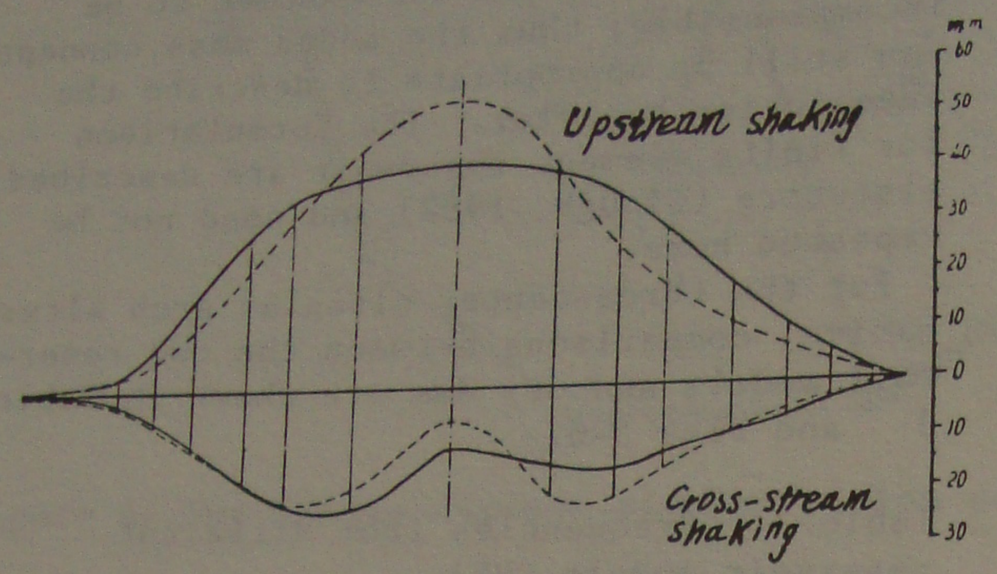

Figure 7a. Displacements of top arch due to the standard response spectrum

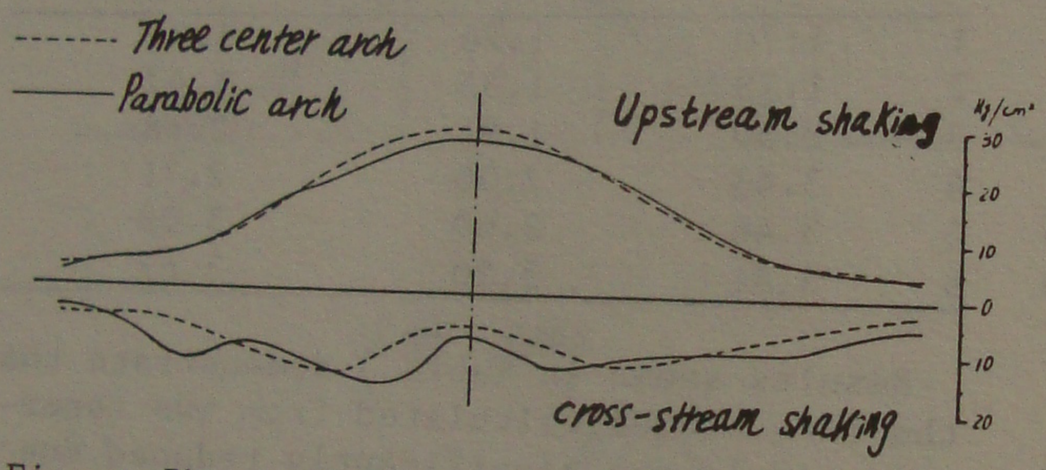

Figure 7b. Arch stresses due to the standard response spectrum

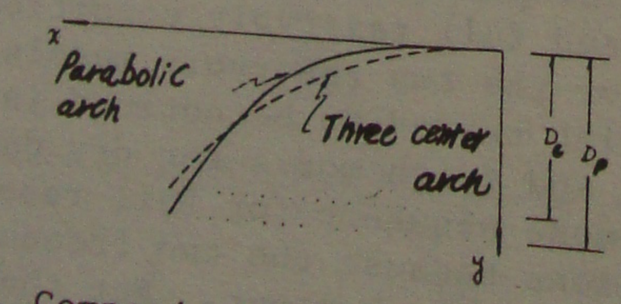

Figure 8. Comparison of parabolic arch and three center circular arch

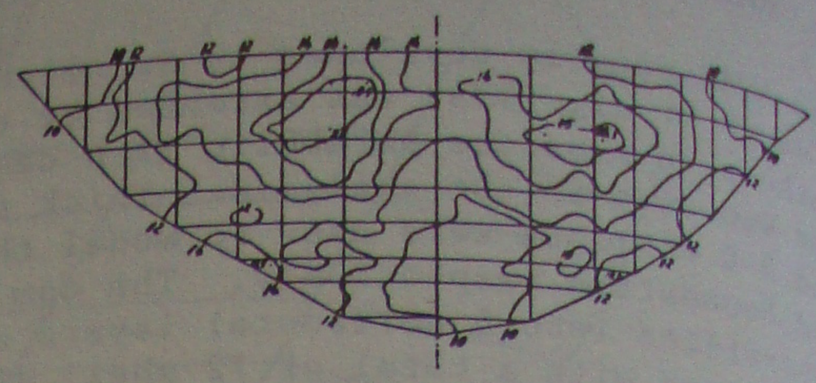

Upstream

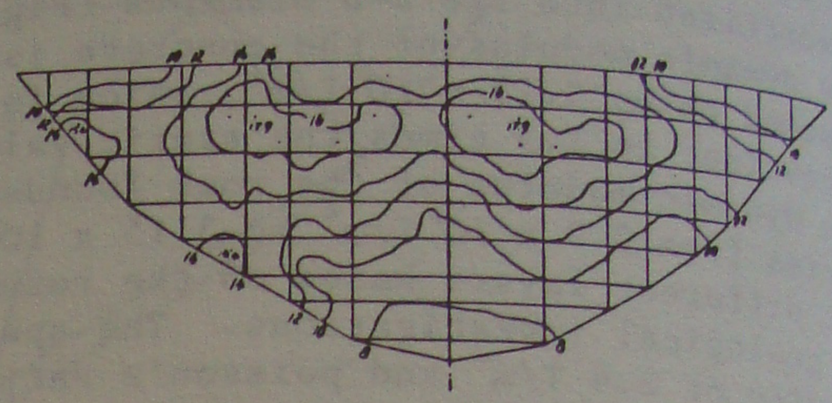

Downstream

Figure 9a. Iso-principal stress(kg/cm^2) due to cross-stream component of the standard response spectrum $(\ddot{v}_g)_{max}$=0.2g

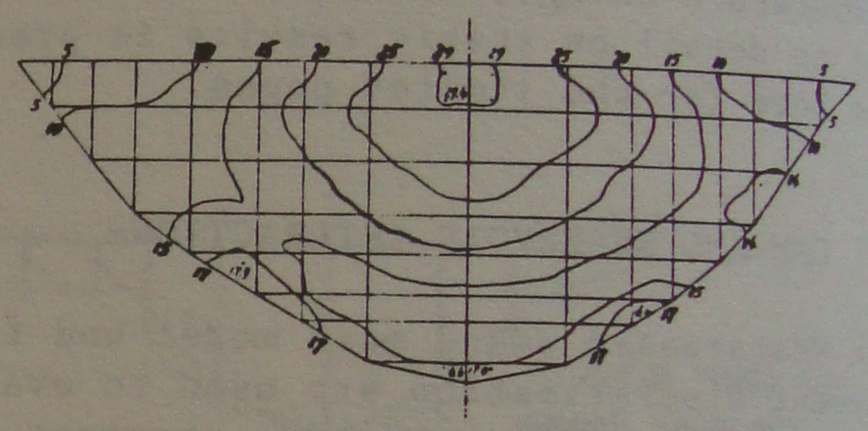

Upstream

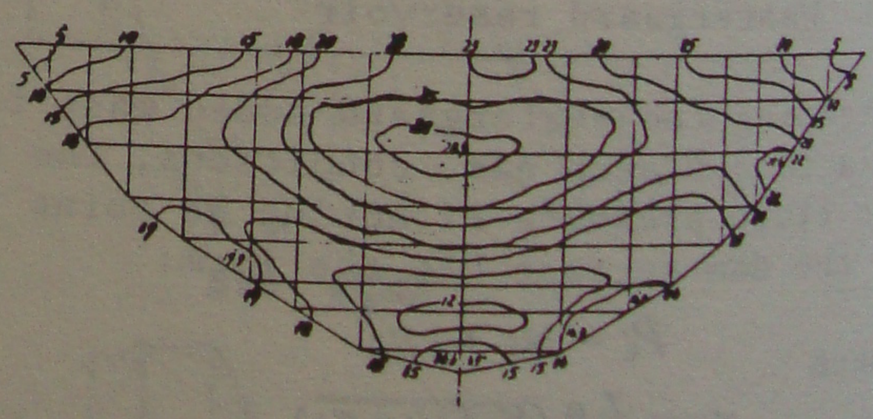

Downstream

Figure 9b. Iso-principal stress(kg/cm^2) due to upstream component of the standard response spectrum $(\ddot{v}_g)_{max}$=0.2g

Westergaard formulation, which was originally derived from gravity dams, will somewhat overestimate the interaction effects for arch dams and gives a safer design. The finite element reservoir model seems more reasonable, as it is able to take the reservoir and abutment geometry into account.

5. EFFECTS OF DAM SHAPE ON EARTHQUAKE RESISTANCE

During the design and investigation courses, two alternative dam shapes have been used for comparison based on the condition of similarity of concrete consumption. A parabolic arch which was proved to have more advantages for abutment stability was compared with a typical three-center circular arch. It was necessary to find out which alternative has better resistance to earthquakes. Table 4 shows a frequency comparison between the two alternatives. It is evident that the parabolic arch shape has lower frequencies for the first 15 modes than the three-center circular arch except the tenth mode.

Table 4. Frequencies of different dam shapes (HZ)

Mode no.	Dam shape	
	Parabolic arch	Three center arch
1	1.22	1.26
2	1.23	1.35
3	1.71	1.94
4	2.29	2.50
5	2.57	2.69
6	2.87	3.20
7	3.10	3.45
8	3.60	3.81
9	3.74	3.92
10	4.03	3.96
11	4.18	4.46
12	4.40	4.60
13	4.54	4.84
14	4.59	4.93
15	5.18	5.25

The displacement and stress response for upstream and cross-stream shakings under the standard response spectrum condition are shown in Fig.7. In comparison with three-center circular arch, the displacement of the parabolic arch is 12.8mm smaller at the center part of the arch, but it is greater at the quarter part for upstream shaking. It finally gives a stress of 2.5kg/cm^2 less than that of the three-center circular. For cross-stream shaking, situation is just the opposite. The parabolic arch has displacement of 1.3mm greater and causes a 2.0kg/cm^2 stress increases compared with the three-center circular arch. It is not surprising that the two alternatives behave differently because of the difference of the curvature distribution. As shown in Fig.8, the parabolic curve has larger curvature at the center arch than at the abutment, and also it has a greater arch height. This curvature difference might explain why the parabolic arch has lower frequencies and better resistance behavior against upstream earthquakes while it has disadvantages in resisting cross-stream shakings. Since the parabolic arch is more beneficial to abutment stability as studies indicated and also to upstream earthquakes, it was finally selected for construction.

6. DAM RESPONSE TO TWO HORIZONTAL EARTHQUAKE COMPONENTS AND THEIR COMBINATIONS

To compare the relative significance of different components the same standard response spectrum of upstream and cross-stream shakings were separately and simultaneously used as the input. The root-mean-square technique was used for combining the total response. The maximum displacements for both components and their combinations are summarized in Table 5. The maximum principal stress contours are shown in Fig.9

Table 5 Unit:mm

Shaking direction	Displacement components	
	Longitudinal (Y-direction)	Transverse (X-direction)
Upstream	42.3 (Crown)	17.1 (Quarter)
Cross-stream	23.2(Neighbor to crown)	11.0 (Quarter)
Combination	45.5(Neighbor to crown)	20.4 (Quarter)

Note:( ) indicates the location

Having studied the patterns of displacement and stress distributions we may make some comments:

(1) For upstream shaking, maximum longitudinal displacements and principal stresses occur at the crown of the top arch. While for cross-stream shaking, they usually occur near the quarter part of the arch. For combinations of the two components, the value and location of the maximum displacement and principal stress are closed to upstream shaking condition.

(2) Contributions to the dam response from different modes indicate that symmetric modes have significant contributions only

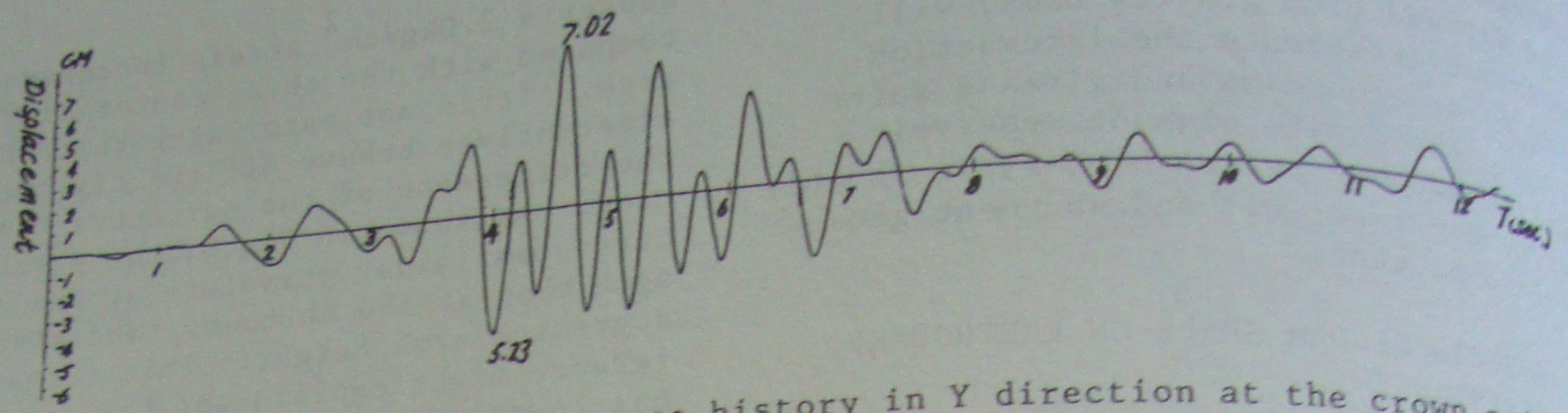

Figure 10. the displacement response history in Y direction at the crown point of top arch due to Park Field earthquake

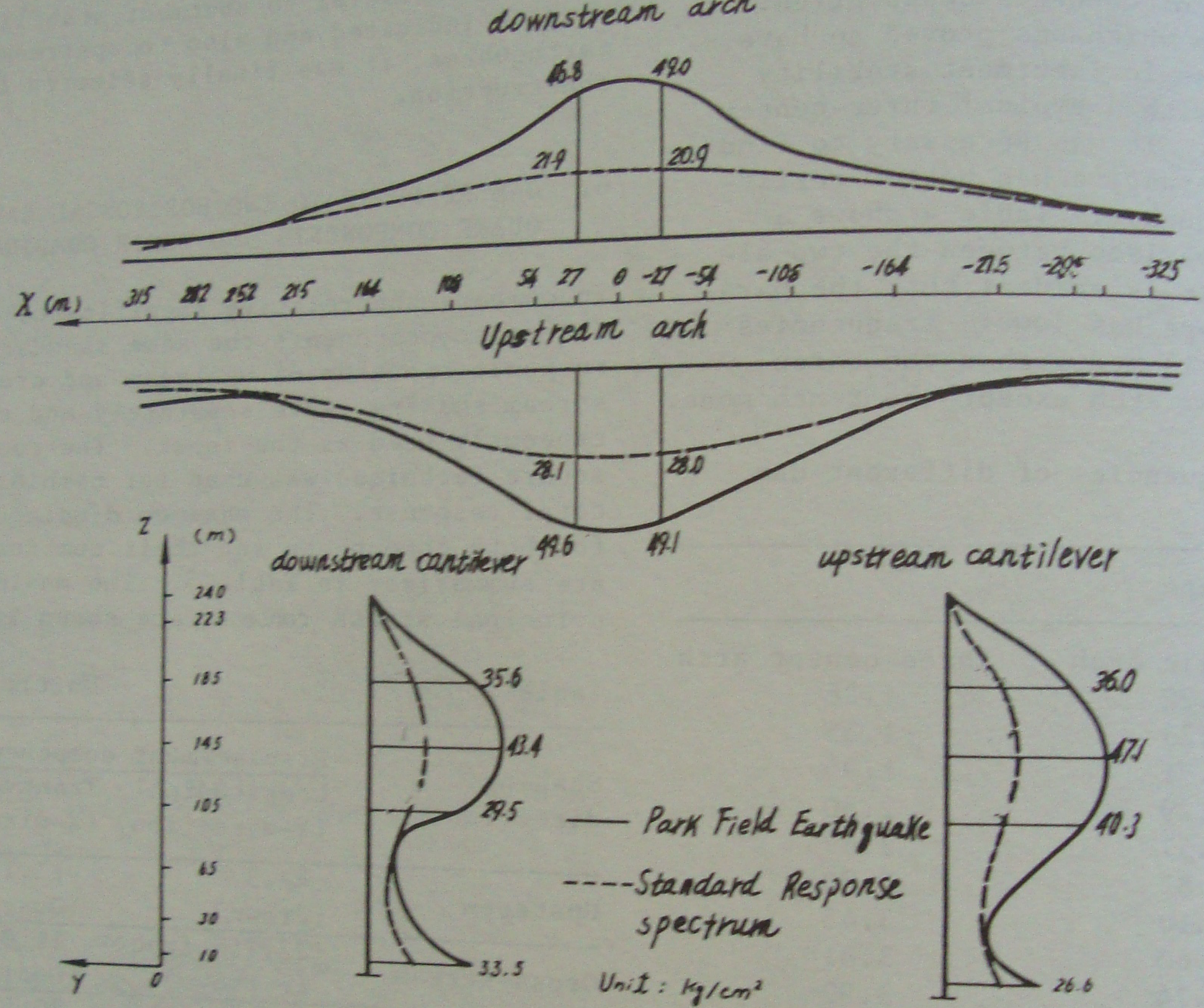

Figure 11. Maximum stresses of arch and crown cantilever

for upstream shakings while nonsymmetric modes are of importance for cross-stream vibration.

(3) In comparing two sets of principal stress contour shown in Fig.9, we find that upstream shaking produces more significant stress than cross-stream vibration and needs more attention in seismic analysis.

7. RESPONSE TO PARK FIELD EARTHQUAKE OF JUNE 27, 1966

The accelerogram of the Park Field Earthquake on June 27, 1966 was proportionally scaled to have a maximum peak acceleration of 0.2g. The dam foundation system shown in Fig.4 and the Westergaard reservoir model were again chosen in analysis. Only upstream excitation was assmued and the first 15 modes of the system were calculated. Fig.10-11 show the displacement response of the crown of top arch and maximum stresses occurring along the arch and crown cantilever. The displacement time history shows an evident contribution of the fundamental and the 4th mode whose frequencies are 1.22HZ and 2.29HZ respectively. Comparing the stress distribution with that obtained from the standard response spectrum, it is evident

that the Park Field earthquake gives a stress about two times of the standard response spectrum results. It is not surprising if we look at the patterns of two spectrum curves shown in Fig.3;vivid differences between the two cause the stress difference, especially in the low frequency range which is more important to high arch dam. Whether the standard response spectrum given in the specification is still suitable for dams higher than 200m needs more investigation involving the study of more earthquake records. On the other hand, results show that for very high arch dams, low frequency components of the earthquake and higher mode contribution of the dam need more attention in the analysis. For the Er-Tan situation, at least the first 12 modes need to be considered, otherwise great errors may occur.

8. DAM SAFETY EVALUATIONS

Based on the National Design Criteria for Arch Dams (For Trial Load Method), the usual loading conditions include hydrostatic, dead weight and temperature changes, while the unusual loading combination includes design earthquake loading added to the usual conditions. Based on the specification requirements, results from the standard response spectrum are used for safety evaluation. Fortunately the maximum tensile stresses due to earthquake loadings occur near the top arch where the static stresses are in compression under the usual loading conditions.The most disadvantageous stresses still occur at the toe and the heel of the cantilever for unusual combination whose values are $-109.8kg/cm^2$ (compressive) at the downstream toe and $+35.3kg/cm^2$ (tensile) at the upstream heel (Table 6).

Table 6. Maximum cantilever stress of Er-Tan dam (kg/cm^2)

	Max.tensile stress	Max.compressive stress
Static	14.5	-90.5
Dynamic	17.8	-17.1
Combination	32.3	-107.6
Max. principal	35.3	-109.8

The compressive strength of the concrete near the base is designed to be $350kg/cm^2$ and tensile strength can be expected to be 35 kg/cm^2 for static loadings. The dynamic strength of concrete is designated to be 30% higher than the static ones. Consequently, the safety factors are 4.1 and 1.3 for compressive and tensile stresses respectively. No criteria of finite element for static and dynamic analysis for arch dams is available at present. However from the results of the study and aseismic design practice world-wide, it is concluded that the dam satisfies the safety requirements for the design earthquake and static conditions as far as the maximum dam stress is concerned.

REFERENCES

Chengdu Design and Exploration Institute of Water Conservancy & Electric Power. 1985. Preliminary design report of Er-Tan power plant.

Clough, R., Raphael,J.& Mojtahedi, S. 1973. ADAP-A computer program for static and dynamic analysis of arch dams, EERC Report No. UCB/EERC-73/14, Univ. of California, Berkeley.

Clough, R.1982. Reservoir interaction effects on the dynamic response of arch dams, Proceedings of US-PRC bilateral workshop on earthquake engineering. Harbin, China.